

# Acid-Catalyzed Hydrogenation during Kerosene Hydrodewaxing over H/ZSM-5

D. C. Longstaff and F. V. Hanson<sup>1</sup>

Department of Chemical and Fuels Engineering, University of Utah, Salt Lake City, Utah 84112

Received December 18, 1995; revised July 23, 1996; accepted July 25, 1996

Hydrogen addition to the products derived from cracking kerosene over H/ZSM-5 was observed at hydrogen pressures between 4.1–8.7 MPa and at 373–390°C. At low pressures, kerosene cracking over H/ZSM-5 yielded typical cracked products: aromatics, as well as low molecular weight saturates and olefins. Endothermic reactor temperature profiles were also observed, indicative of cracking reactions. At high hydrogen partial pressures product selectivity was altered in that kerosene cracking gave high yields of low molecular weight paraffins and low yields of olefins and aromatics. Reactor temperature profiles were exothermic, indicative of hydrocracking reactions. A mechanism for acid catalyzed hydrogenation is suggested. Although hydrogenation was not observed at lower hydrogen pressures, hydrogen proved beneficial in maintaining catalyst activity at a stable level. Lost catalyst activity was restored by maintaining the catalyst under static hydrogen at 1.4 MPa and 370°C for 16 h. © 1996 Academic Press, Inc.

## INTRODUCTION

Acid catalyzed dehydrogenation has been reported (1, 2) and is coupled with the formation of methane during isobutane cracking (3). This reaction mechanism is depicted in Fig. 1. Methane and hydrogen formation during isobutane cracking have been suggested by McVickers *et al.* (4, 5) to be the result of a surface catalyzed free radical reaction. Although the formation of methane in isobutane cracking is suggestive of a radical mechanism, it is generally accepted that these products result from protolytic cracking involving a carbonium-like transition state where a proton from a pristine Brønsted acid site (1, 6) interacts with isobutane.

It is recognized that zeolites lack the acidity to protonate olefins to form carbenium ions and to protonate paraffins to form carbonium ions (7–9). However, the transition states in the bimolecular and monomolecular cracking mechanisms bear some resemblance to carbenium and carbonium ions, respectively. For that reason, the terms carbenium ions

(Fig. 2a) and carbonium ions (Fig. 2b) are used here to indicate transition states that bear resemblance to the respective ions but are lacking in complete separation of positive and negative charges.

Whether the conventional bimolecular (carbenium ion-like) transition state or the more recently reported monomolecular (carbonium ion-like) transition state predominates during cracking is determined by five factors: (1) temperature (1) (>350°C); (2) hydrocarbon pressure (1) (<10 kPa); (3) conversion (1) (<5–10%); (4) catalyst acidity; and (5) catalyst structure. These five factors act to change the relative concentrations of olefins available to participate in the bimolecular cracking mechanism.

High temperature discourages carbenium ion cracking because the adsorption of olefins on pristine Brønsted acid sites is suppressed (10). Low hydrocarbon partial pressure and low conversion both favor carbonium ion cracking by decreasing the concentration of olefins that are available to participate in the bimolecular cracking mechanism (1). Catalyst acidity and pore structure affect the mechanism by either discouraging the interaction of olefins with weakly acidic acid sites or by hindering hydride exchange in the bimolecular cracking mechanism (11, 12) which is the rate determining step for alkane cracking (1). Any additional reaction or catalytic variable capable of changing the relative concentration of olefins or their ability to form a carbenium ion-like transition state will also influence the relative importance of the mono- and the bi-molecular cracking mechanisms.

Research has been conducted (13) to determine if hydrogen influences cracking selectivity. The results of this research has indicated that low pressure hydrogen exhibits little influence on catalytic cracking (13); however, more recent research has shown that ethylene (14, 15), propylene (16), and even benzene (17) can be hydrogenated at moderate hydrogen pressures by acid catalysts in the absence of a conventional hydrogenation function such as a metal cation.

Hydrogenation has also been observed during the cracking of kerosene (18) and *n*-heptane (19–20). It has been suggested (18, 19) that olefins are hydrogenated by hydride

<sup>1</sup> Send proofs to: Francis V. Hanson, Department of Chemical & Fuels Engineering, 3290 MEB, University of Utah, Salt Lake City, UT 84112. Phone: (801)581-6591 or (801)581-7187; Fax: (801)581-3344; E-mail: francis.hanson@m.cc.utah.edu.

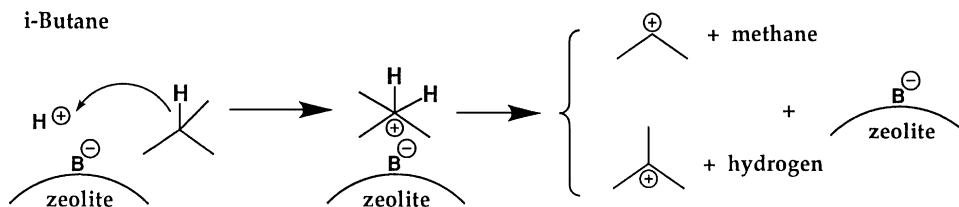


FIG. 1. Carbonium ion cracking of isobutane.

transfer from molecular hydrogen to olefins adsorbed as carbenium ions (18, 19).

The objective of this research was to explore the effect of hydrogen on cracking activity and selectivity during kerosene hydrodedewaxing over H/ZSM-5.

## METHODS

Zeolite ZSM-5 was prepared to contain a 30:1 Si/Al ratio according to the Type A synthesis (21). Scanning electron microscopy (SEM) indicated that the zeolite consisted of 5  $\mu\text{m}$  agglomerates 0.5  $\mu\text{m}$  crystallites. The air-calcined zeolite was converted to the protonic form by three, 24-h, ammonium nitrate exchanges at 75°C followed by an air calcination at 538°C. The zeolite was pelleted in a pellet press at 415 MPa and then crushed and sized between 14 and 30 mesh. The liquid feed was a waxynaphthenic kerosene blend of Altamont and Wyoming Sweet crudes.

A 2.0-g zeolite sample was loaded into a 1.27 cm ID reactor tube which contained an axially positioned thermowell. Alumina pellets were placed in the reactor above and below the zeolite sample to respectively facilitate preheater heat transfer and to provide support for the catalyst bed. The catalyst bed was approximately 2.5-cm long.

The kerosene was fed into the reactor with a metering pump and the hydrogen flow to the reactor was controlled with a mass flow controller. Liquid samples were collected

in a liquid receiver at ambient temperature and volatiles were collected in a liquid nitrogen trap at  $-197^\circ\text{C}$  for approximately 1 h. The contents of the vapor and liquid collectors were weighed to complete the mass balance.

The methane yield was determined by gas chromatographic analysis obtained during the steady state mass balance because methane does not condense at  $-197^\circ\text{C}$ . The methane-to-ethane ratio obtained from this analysis was used to determine the total methane yield.

Gas samples were analyzed on a Hewlett Packard 5730A gas chromatograph containing a 6.1 m  $\times$  0.32 cm column packed with Chromosorb 102. Liquid samples were analyzed on a Hewlett Packard 5730A gas chromatograph containing 10-m wide bore capillary column coated with 5% phenyl-methylsilicone.

A waxy naphthenic kerosene (138–330°C, M.W. = 182 g/mol) was used as a feedstock in a series of experiments in which the hydrogen partial pressure was varied from 0.3 to 8.7 MPa. The operating conditions employed to hydrodedewax kerosene are outlined in Table 1. The kerosene WHSV ranged from 11.4–12.1  $\text{h}^{-1}$  in these experiments. The hydrogen feed rate was varied to keep the partial pressure of hydrocarbon feed constant at about 0.24 MPa (1800 torr). The kerosene feed was completely vaporized at reaction conditions. A detailed explanation of the procedures is given by Longstaff (18).

## RESULTS AND DISCUSSION

Reactor temperature profiles taken at hydrogen partial pressures of 0.3 MPa, 4.1 MPa, and 8.7 MPa are presented in

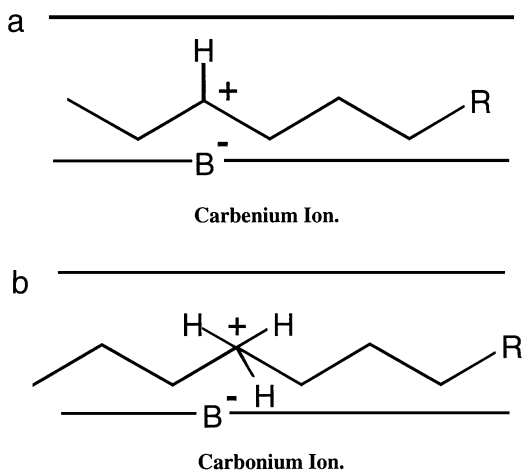


FIG. 2. Examples of carbenium and carbonium ions.

TABLE 1

Operating Conditions Employed to Hydrodedewax Kerosene

| Run number | $P_{\text{total}}$ , MPa | $P_{\text{H}_2}$ , MPa | T, $^\circ\text{C}$ | WHSV, $\text{h}^{-1}$ |
|------------|--------------------------|------------------------|---------------------|-----------------------|
| 83         | 0.5                      | 0.3                    | 374                 | 11.4                  |
| 82         | 1.4                      | 1.2                    | 376                 | 11.6                  |
| 81         | 2.2                      | 2.0                    | 375                 | 11.5                  |
| 80         | 3.3                      | 3.0                    | 376                 | 11.8                  |
| 79         | 4.3                      | 4.1                    | 376                 | 11.7                  |
| 78         | 5.2                      | 4.9                    | 379                 | 12.1                  |
| 77         | 6.5                      | 6.3                    | 377                 | 11.9                  |
| 73         | 9.0                      | 8.7                    | 378                 | 11.9                  |

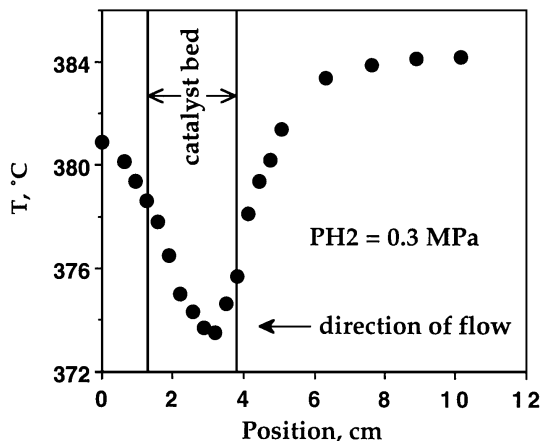


FIG. 3. Reactor temperature profile ( $P_{H_2} = 0.3$  MPa).

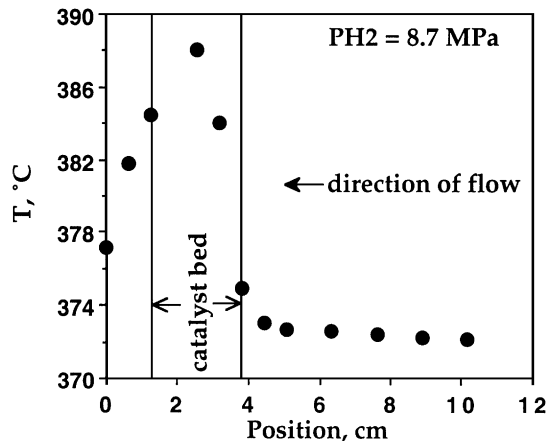


FIG. 5. Reactor temperature profile ( $P_{H_2} = 8.7$  MPa).

Figs. 3 through 5, respectively. The temperature profile data in Fig. 3 indicates that there is an endothermic temperature profile through the catalyst bed at low hydrogen partial pressure. This is expected because cracking is an endothermic reaction. Increasing the hydrogen partial pressure led to the formation of an exotherm at the catalyst bed outlet (Fig. 4). The exotherm present in the catalyst bed outlet at a hydrogen partial pressure of 4.1 MPa expanded to fill the entire reactor bed when hydrogen partial pressure was increased to 8.7 MPa (Fig. 5). This suggests that the products of kerosene cracking were being hydrogenated.

It was estimated that the volumetric heat capacity of the feed increased by a factor of 2.5 between the run conducted at a hydrogen partial pressure of 0.3 MPa and the run conducted at a hydrogen partial pressure at 8.7 MPa. Because of this increase, the influence of the heat of reaction on the upstream temperature profile was minimized at the higher pressure. This is because of the greater capacity of the feed to cool the reactor inlet at higher pressures (Fig. 5) relative to the feed's capacity to heat the reactor inlet at lower pressures (Fig. 3).

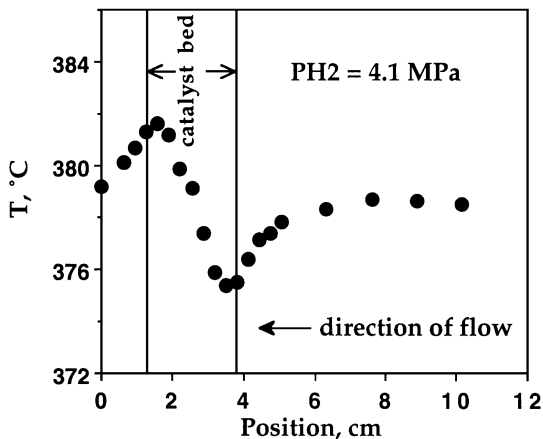


FIG. 4. Reactor temperature profile ( $P_{H_2} = 4.1$  MPa).

The possibility that the observed exotherms were an artifact related to the increase in the heat capacity of the feed with increasing pressure was considered. An experiment was conducted in which hydrogen was replaced with nitrogen which has the same molar heat capacity as hydrogen. The formation of an exotherm at the reactor outlet was not observed with nitrogen at 4 MPa as it was in the presence of hydrogen (Fig. 4).

Confirmation of hydrogenation is provided in Fig. 6 which displays the estimated hydrogen-to-carbon ratio of the products boiling below  $C_{10}$  plotted versus hydrogen partial pressure. This ratio was estimated by summing the hydrogen-to-carbon ratio of the individual gas and liquid products collected during the mass balance. As the hydrogen partial pressure was increased there was a clear increase in the hydrogen content of the products. This hydrogenation led to the exothermic temperature profiles that are displayed in Figs. 4-5.

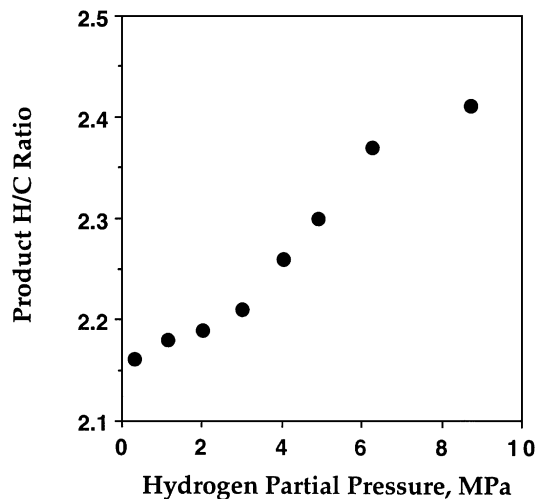


FIG. 6. The effect of hydrogen partial pressure on total product H/C ratio.

TABLE 2  
Product Yields<sup>a</sup> versus Hydrogen Partial Pressure

| $P_{H_2}$ , MPa | $C_2-C_4$ | $C_1$ | $C_2$ | $iC_4/nC_4$ | H/C  | Conversion |
|-----------------|-----------|-------|-------|-------------|------|------------|
| 0.3             | 52.7      | 0.29  | 3.50  | 0.42        | 2.16 | 43.4       |
| 1.2             | 42.9      | 0.81  | 3.82  | 0.35        | 2.18 | 48.7       |
| 2.0             | 35.9      | 1.37  | 4.37  | 0.47        | 2.19 | 45.5       |
| 3.0             | 37.4      | 2.50  | 5.84  | 0.49        | 2.21 | 43.1       |
| 4.1             | 29.4      | 3.32  | 6.55  | 0.45        | 2.26 | 48.1       |
| 4.9             | 20.9      | 3.57  | 7.10  | 0.43        | 2.30 | 49.2       |
| 6.3             | 10.2      | 4.82  | 7.98  | 0.48        | 2.37 | 54.2       |
| 8.7             | 2.1       | 6.36  | 10.13 | 0.75        | 2.41 | 59.6       |

<sup>a</sup> moles/100 moles of feed cracked.

Product yields with respect to hydrogen partial pressure are presented in Table 2. The yield of  $C_2-C_4$  olefins is displayed with respect to hydrogen partial pressure in Fig. 7 and shows that hydrogen partial pressure reduced the yield of olefins to almost zero. At the highest hydrogen partial pressure only traces of olefins were present in the products.

The decrease in selectivity to olefins could be the result of either olefin hydrogenation or an accelerated conversion of olefins to aromatics and paraffins by means of hydrogen transfer reactions. The yield of  $C_6-C_9$  aromatics is displayed in Fig. 8. The 50% decrease in aromatic yield with increasing hydrogen pressure indicates that the reduced selectivity to olefins is not the result of increased hydrogen transfer reactions. The decrease in aromatic yields is therefore attributed to fewer aromatics being formed from olefins because the olefin concentration is decreasing due to hydrogenation.

Aromatics are produced from olefins through a series reaction scheme (22). If 8.7 MPa hydrogen partial pressure leads to almost total hydrogenation of olefins it is expected that the aromatic yield should also have been almost zero. It was not because the olefin concentration in the catalyst bed

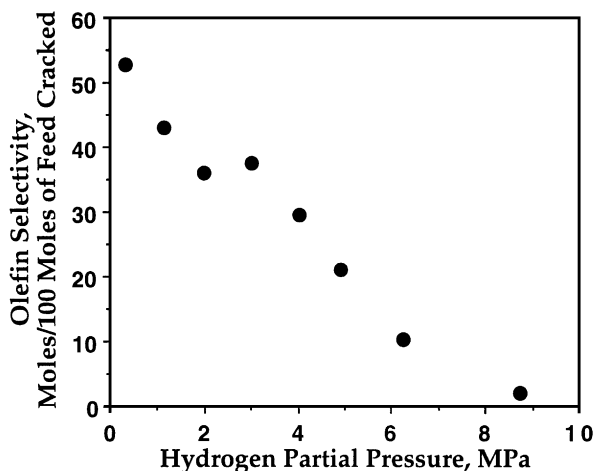


FIG. 7. The effect of hydrogen partial pressure on the selectivity to  $C_2-C_4$  olefins.

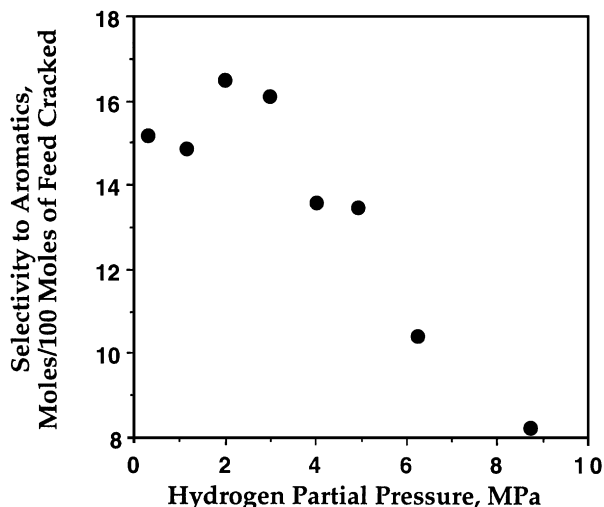


FIG. 8. The effect of hydrogen partial pressure on the selectivity to aromatics.

probably reached levels high enough for the observed aromatic formation to occur. However, the rate of olefin hydrogenation was significant enough for almost total conversion of olefins to occur prior to the outlet of the catalyst bed.

Hydrogenation of olefins through a carbenium ion-like transition state is probably occurring by a hydrogen transfer mechanism in which the hydride donor to the carbenium ion is not a saturated hydrocarbon, but a hydrogen molecule (18–20). This mechanism is simply the reverse of acid catalyzed hydrogenation which has been previously reported (1–3). Normally when a carbenium ion abstracts a hydride from a paraffin, a new carbenium ion is formed which can isomerize and/or crack. This conventional hydride abstraction mechanism is depicted in Fig. 9a. However, in this instance (Fig. 9b) a carbenium ion abstracts a hydride ion

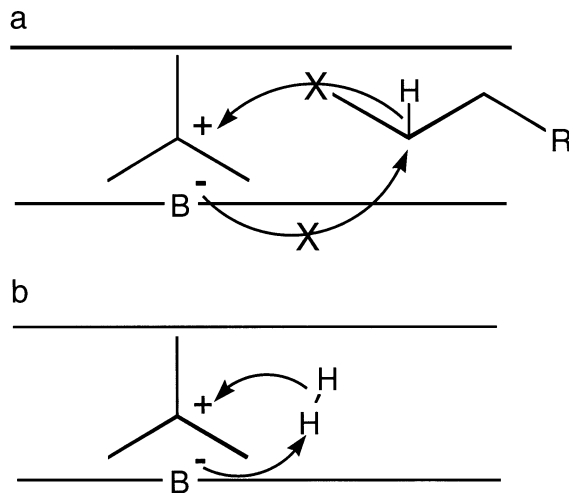


FIG. 9. Transition state selectivity during hydride transfer: (a) hindered due to the size of the transition state; (b) not hindered.

from hydrogen and the pristine Brønsted acid site is regenerated.

Cracking in wide-pore zeolites and silica-alumina yields high isoparaffin-to-normal paraffin ratios. This is because tertiary carbenium ions abstract hydrides as much as 10 times faster than secondary carbenium ions (11). However, in medium pore zeolites, such as ZSM-5, the smaller pore dimensions hinder the formation of the transition state between tertiary carbenium ions and paraffins (Fig. 9a). For that reason, isoparaffin-to-normal paraffin ratios on ZSM-5 are low. If carbenium ions are being saturated by abstracting hydride ions from molecular hydrogen (Fig. 9b), the isoparaffin-to-normal paraffin ratio should increase. This is because the required transition state for hydride transfer from molecular hydrogen to a tertiary carbenium ion will be significantly less hindered than it is when the source of the hydride is a paraffin. This phenomena was observed with respect to the ratio of isobutane to *n*-butane (Fig. 10) and to the ratio of isopentane to *n*-pentane. Additional experiments were conducted in which nitrogen and helium were substituted for hydrogen at hydrogen partial pressures of 1.4 MPa. These results indicate that the presence of hydrogen led to a 10–15% increase in the isobutane-to-normal butane ratio (18) at 1.4 MPa.

High hydrogen partial pressures led to additional changes in product selectivity which are presented in Figs. 11 and 12. The carbon number distribution of products produced at hydrogen partial pressures of 1.2 MPa and 8.7 MPa is presented in Fig. 11 and in Table 3. As hydrogen partial pressure increased the selectivity shifted from +C<sub>5</sub> to C<sub>1</sub>–C<sub>3</sub> products.

The effect of hydrogen partial pressure on the reaction selectivity is further illustrated in Fig. 12 in which the yield of methane and C<sub>2</sub> products with respect to hydrogen par-

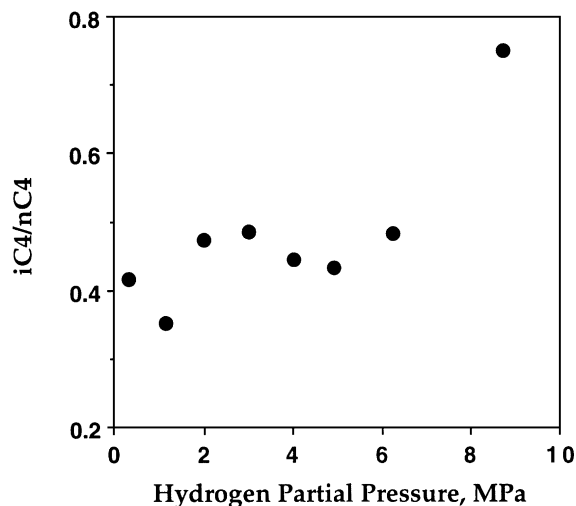


FIG. 10. The effect of hydrogen partial pressure on the *i*-butane-to-*n*-butane ratio.

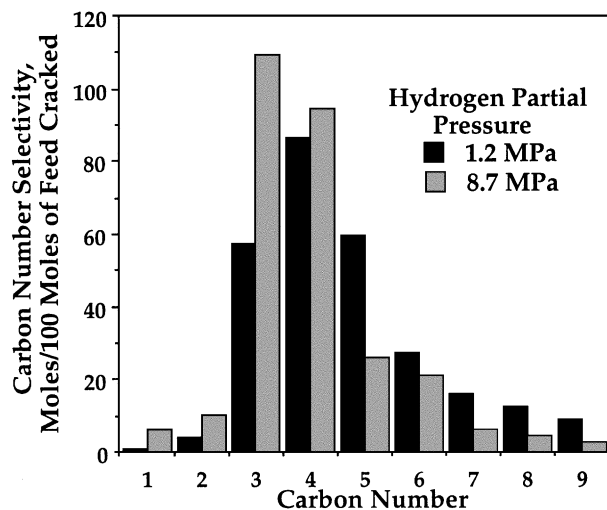


FIG. 11. The effect of hydrogen partial pressure on the carbon number distribution.

tial pressure is plotted. The change in selectivity to methane and C<sub>2</sub> suggest a fundamental shift of mechanism as the hydrogen partial pressure increased. Extrapolating the data for C<sub>2</sub> selectivity to zero hydrogen partial pressure yields the selectivity of C<sub>2</sub> in the absence of hydrogen which is about 3 moles of C<sub>2</sub> for every 100 moles of feed that were cracked. This value reflects the slight tendency of ethylene to be produced in the bimolecular cracking mechanism. Because methane cannot be formed in the conventional bimolecular cracking mechanism, the selectivity of methane at zero hydrogen partial pressure was zero.

Methane production during cracking of butanes (1, 4, 5, 23–26), neopentane (10, 24), hexanes (1, 12), and *n*-heptane (12) has been associated with the monomolecular cracking mechanism. The predominance of the monomolecular

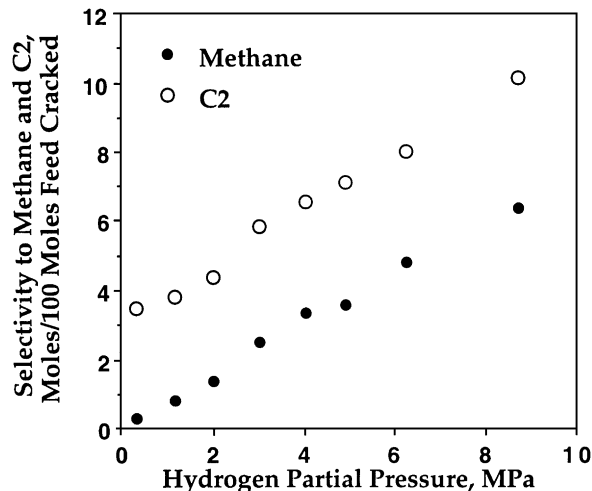


FIG. 12. The effect of hydrogen partial pressure on the selectivity to C<sub>1</sub> and C<sub>2</sub>.

TABLE 3  
Carbon Number Distribution<sup>a</sup> versus  
Hydrogen Partial Pressure

| $P_{H_2}$ : Carbon number | 1.2 MPa | 8.7 MPa |
|---------------------------|---------|---------|
| C <sub>1</sub>            | 0.8     | 6.4     |
| C <sub>2</sub>            | 3.8     | 10.1    |
| C <sub>3</sub>            | 57.1    | 109.1   |
| C <sub>4</sub>            | 86.3    | 94.4    |
| C <sub>5</sub>            | 59.7    | 25.9    |
| C <sub>6</sub>            | 27.4    | 21.0    |
| C <sub>7</sub>            | 16.0    | 6.2     |
| C <sub>8</sub>            | 12.7    | 4.4     |
| C <sub>9</sub>            | 9.2     | 2.6     |

<sup>a</sup> moles/100 moles of feed cracked.

mechanism during cracking depends on factors such as the acidity of the catalyst, high reaction temperature, low olefin conversion, or low hydrocarbon partial pressure. These are factors which decrease the concentration of olefins (1) or their ability to interact with acid sites. The conditions of hydrocarbon concentration, conversion, and temperature used in this study should strongly favor the carbenium ion cracking mechanism. However, the hydrogenation of olefins occurring at higher hydrogen partial pressures reduced the concentration of olefins. This led to an increase in the carbonium ion mechanism relative to the carbenium ion mechanism and the observed increase in the selectivity to C<sub>1</sub>–C<sub>3</sub> products.

In addition to selectivity changes, increasing hydrogen pressure resulted in higher kerosene conversion. Feed conversion was defined as the amount of kerosene converted to material boiling below *n*-decane as determined from gas chromatography. Gas chromatography of the kerosene feed indicated that no more than 48% of the feed consisted of normal paraffins, with the balance presumably being naphthenes. Because ZSM-5 is selective for cracking paraffins in the presence of naphthenes no more than 48% conversion of the kerosene was expected. However, kerosene conversion rose from 43 to 60% (Fig. 13) as the hydrogen partial pressure was increased from 0.3 to 8.7 MPa. Although the reactor temperature increased by 7–8°C due to heat generated by exothermic hydrogenation reactions, the majority of the conversion increase is attributed to a decrease in transition state selectivity with increasing hydrogen partial pressure.

Transition shape selectivity during cracking has been reported (27). The constraint index, that is, the ratio of the rates of *n*-hexane to 3-methylpentane cracking, over H/ZSM-5 decreases from 12 to 1 when the temperature is raised from about 200°C to 500°C. The high constraint index for ZSM-5 at low temperatures is attributed to transition state selectivity (1, 28) wherein hydride transfer from 3-methylpentane to olefins is hindered because there is

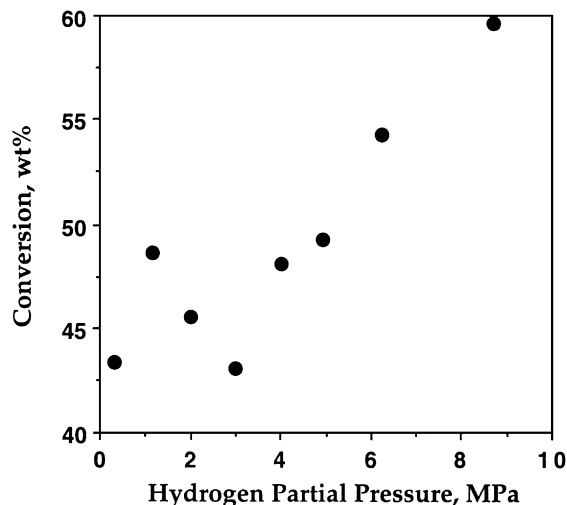


FIG. 13. The effect of hydrogen partial pressure on the conversion of kerosene.

insufficient room in the pores of H/ZSM-5 for a molecule of the methyl substituted paraffin to approach a carbenium ion. The decrease in the constraint index with increasing temperature indicates a shift from the bimolecular to the monomolecular cracking mechanism. This is because there is a shift from a mechanism initiated by a constrained bimolecular hydride transfer to an unconstrained monomolecular mechanism initiated by a proton transfer from the zeolite to 3-methylpentane.

It is expected that a certain portion of the naphthenic molecules in the kerosene feed were able to diffuse into the pores of ZSM-5. During conditions when the bimolecular mechanism predominates these molecules are not converted because they are too large to form a transition state with olefins in order to transfer hydride ions (Fig. 14a). However, when the monomolecular mechanism predominates these molecules are able to directly accept protons

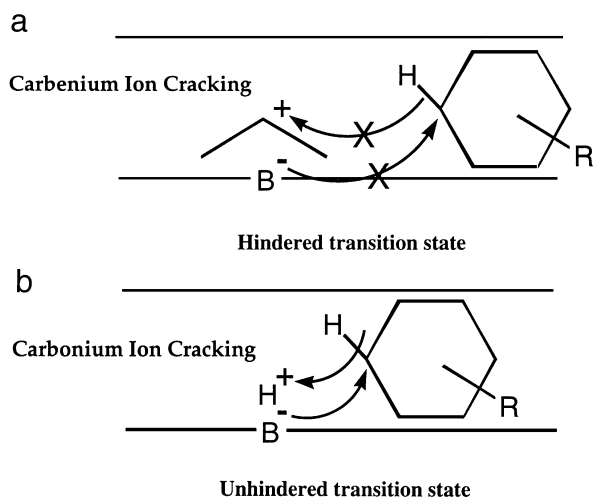


FIG. 14. Transition state selectivity during naphthene cracking.

from pristine Brønsted sites and form a carbonium ion-like transition state (Fig. 14b).

The higher kerosene conversion observed with increasing hydrogen partial pressures is not attributed to higher catalyst activity. Instead, it is attributed to changes in transition state selectivity which permit a greater fraction of the kerosene to be cracked. This changing transition state selectivity affected naphthenes which were small enough to diffuse into ZSM-5 but were too large to approach carbenium ions to transfer hydride ions.

It is predicted that an increase in hydrogen partial pressure will result in a decrease in the constraint index over ZSM-5 as the cracking mechanism changes from bimolecular cracking to monomolecular cracking.

Even if some naphthenes are able to form carbenium ion-like transition states, they will still crack much more slowly than paraffins. This is because of poor overlap between the empty  $p$ -orbital of the positively charged carbon atom and the C-C bond of the adjoining carbon atom in the naphthenic ring (29). Because carbonium ion cracking does not require overlap between an empty  $p$ -orbital and a C-C bond, carbonium ion cracking of naphthenes is not hindered to the same degree as carbenium ion cracking. Therefore a change of mechanism from carbenium ion cracking to carbonium ion cracking should lead to a substantial increase in the cracking rate of naphthenes relative to paraffins.

The beneficial effects of hydrogen on catalyst activity has been exploited to regenerate H/ZSM-5 following reactor upsets (30). This was confirmed in this research in that catalyst activity could be restored by maintaining the catalyst for 16 h in static hydrogen at 1.4 MPa and 370°C.

There has been some debate on whether methane produced during cracking results from a carbonium ion-like transition state or a radical type cracking mechanism (31–33). The active site for the radical mechanism has been postulated to be electron acceptor sites which have been shown to be present in ZSM-5 (34) and on silica-alumina catalysts (35). Treatment of ZSM-5 (34) and silica-alumina with hydrogen (36) has been shown to reduce the concentration of radical species by over an order of magnitude. If increased methane selectivity was the result of a radical mechanism catalyzed by electron acceptor sites, then increasing the hydrogen pressure should reduce the yield of methane. However, the opposite trend was observed.

## CONCLUSIONS

High pressure hydrogen exhibits a significant role in catalytic cracking at 370–400°C. Kerosene conversion, selectivity to methane and C<sub>2</sub> hydrocarbons increased as the hydrogen partial pressure was increased from 0.3 to 8.7 MPa. Almost complete hydrogenation of olefins occurred. The aromatics yield was also reduced at higher pressures but not as dramatically as the yield of olefins.

Hydrogen served as a source of hydrides for olefins through a carbenium ion-like transition state. This reduced the interaction between olefins and acid sites which suppressed carbenium ion cracking. Because carbenium ion cracking is suppressed pristine Brønsted acid sites are able to participate in carbonium ion cracking which leads to an increase in the yield of C<sub>1</sub>–C<sub>3</sub> products.

The ability of hydrogen to reduce the concentration of electron acceptor sites suggests that high pressure hydrogen should suppress radical-type products; however, the opposite trend was observed which suggests that radical type products, such as methane, are the result of carbonium ion cracking.

## ACKNOWLEDGMENTS

The Wright Aeronautical Laboratories at Wright-Patterson Air Force Base is thanked for financial support of this work. Dr. Werner O. Haag and Professor Alex G. Oblad are thanked for helpful discussions.

## REFERENCES

1. Haag, W. O., and Dessau, R. M., in "Proceedings, Int. Congr. Catal. 8th, Berlin, West Germany," Vol. 2, p. 305, (1984); Haag, W. O., and Lago, R. M., *Stud. Surf. Sci. Catal.* **60**, (1991).
2. Brenner, A., and Emmett, P., *J. Catal.* **75**, 410 (1982).
3. Lombardo, E. A., and Hall, W. K., *J. Catal.* **112**, 565 (1988).
4. McVicker, G. B., Kramer, G. M., and Ziemiak, J. J., *J. Catal.* **83**, 286 (1983).
5. Kramer, G. M., McVicker, G. B., and Ziemiak, J. J., *J. Catal.* **92**, 355 (1985).
6. Corma, A., Planelles, J., Sanchez-Marin, J., and Tomas, F., *J. Catal.* **93**, 30 (1985).
7. Kazansky, V. B., and Senchenya, I. N., *J. Catal.* **119**, 108 (1989).
8. Aronson, M. T., Gorte, R. J., Farneth, W. E., and White, D., *J. Am. Chem. Soc.* **111**, 840 (1989).
9. Haw, J. F., Richardson, B. R., Oshiro, I. S., Lazon, N. D., and Speed, J. A., *J. Am. Chem. Soc.* **111**, 2052 (1989).
10. Lombardo, E. A., Pierantozzi, R., and Hall, W. K., *J. Catal.* **110**, 171 (1988).
11. Greensfelder, B. S., Voge, H. H., and Good, G. M., *Ind. Eng. Chem.* **41**(11), 2573 (1949).
12. Wielers, A. F. H., Vaarkamp, M., and Post, M. F. M., *J. Catal.* **127**, 51–66 (1991).
13. Greensfelder, B. S., and Voge, H. H., *Ind. Eng. Chem.* **38**(10), 1033 (1946).
14. Gadalla, A. M., Chan, T., and Anthony, R. G., *Int. J. Chem. Kin.* **15**, 759 (1983).
15. Kanai, J., Martens, J., and Jacobs, P. A., *J. Catal.* **133**, 527 (1992).
16. Sano, T., Okabe, K., Shoji, H., Saito, K., Yasumoto, Y., Hagiwara, H., and Takaya, H., *Bull. Chem. Soc. Jpn.* **58**, 3371 (1985).
17. Sano, T., Okabe, K., Hagiwara, H., and Takaya, H., *J. Mol. Catal.* **40**, 113 (1987).
18. Longstaff, D. C., "Shape Selective Hydrodewaxing of Jet Fuel Boiling Range Distillates," M.S. thesis, University of Utah, 1988.
19. Meusinger, J., Liers, J., Mosch, A., and Reschetilowski, W., *J. Catal.* **148**, 30 (1994).
20. Meusinger, J., and Corma, A., *J. Catal.* **152**, 189 (1995).
21. Derouane, E. G., Detremmerie, S., Gabelica, Z., and Blom, N., *Appl. Catal.* **1**, 201 (1981).
22. Chang, C. D., Chu, C.T.W., and Socha, R. F., *J. Catal.* **86**, 289 (1984).

23. Stefanadis, C., Gates, B. C., and Haag, W. O., *J. Mol. Catal.* **67**, 363 (1991).
24. Engelhardt, J., and Hall, W. K., *J. Catal.* **125**, 472 (1990).
25. Shigeishi, R., Garforth, A., Harris, I., and Dwyer, J., *J. Catal.* **130**, 423 (1991).
26. Ono, Y., and Kanae, K., *J. Chem. Soc. Faraday Trans.* **87**, 663 (1991).
27. Frilette, V. J., Haag, W. O., and Lago, R. M., *J. Catal.* **67**, 218 (1981).
28. Haag, W. O., Lago, R. M., and Weisz, P. B., *Faraday, Disc., J. Chem. Soc.* **72**, 317 (1982).
29. Haag, W. O., personal communication.
30. Donnelly, J. P., and Green, J. R., *Oil & Gas J.* **78**(43), 77 (1980).
31. Lombardo, E. A., and Hall, W. K., *J. Catal.* **112**, 565 (1988).
32. Kramer, M., and McVicker, G. B., *J. Catal.* **115**, 608 (1989).
33. Hall, W. K., Lambardo, E. A., and Engelhardt, J., *J. Catal.* **115**, 611 (1989).
34. Shih, S., *J. Catal.* **79**, 390 (1983).
35. Dollish, F., and Hall, W. K., *J. Phys. Chem.* **69**, 4402 (1965).
36. Hall, W. K., *J. Catal.* **1**, 53 (1962).